Electronic Supplementary Information

DON encapsulated carbon dot-vesicle conjugate in therapeutic intervention of lung adenocarcinoma by dual targeting of CD44 and SLC1A5

Afreen Zaman, Aparajita Ghosh, Anup Kumar Ghosh and Prasanta Kumar Das*

School of Biological Sciences, Indian Association for the Cultivation of Science Jadavpur, Kolkata – 700032, India.

*To whom correspondence should be addressed: bcpkd@iacs.res.in

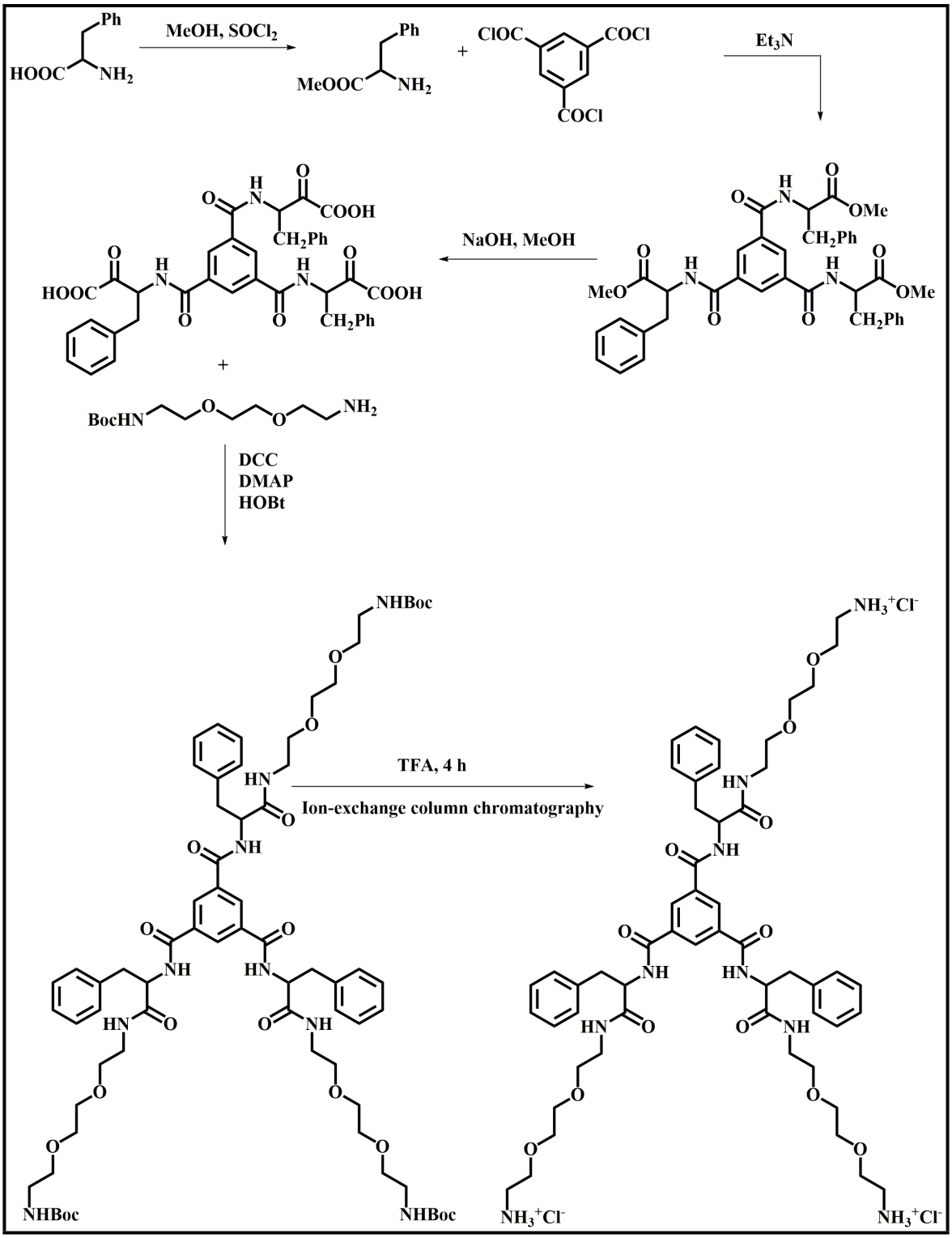

Scheme S1. Synthetic scheme of TMAV.

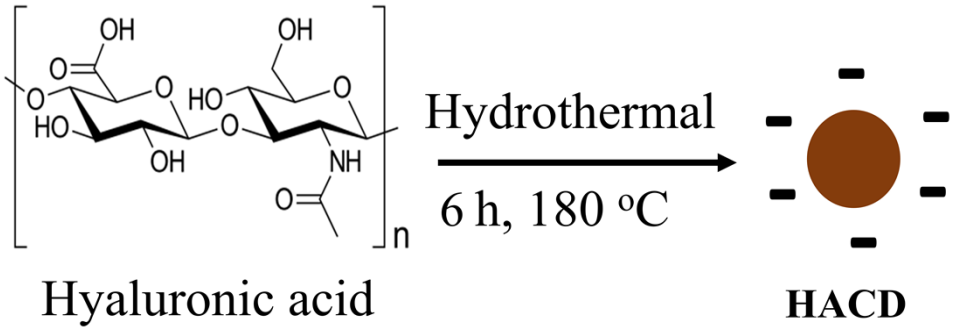

Hyaluronic acid

HACD

Scheme S2. Synthetic scheme of HACD.

Experimental details

Materials. Sodium hyaluronate and trimesoyl chloride were procured from BLD Pharma. Silica gel of 100−200 mesh and 60−120 mesh, L-phenylalanine, *N*,*N*-dicyclohexylcarbodiimide (DCC), 4-*N*,*N*-(dimethylamino) pyridine (DMAP), *N*-hydroxybenzotriazole (HOBT), trifluoroacetic acid (TFA), triethylamine (Et3N) and all other solvent and chemicals were purchased from SRL, India. 6-Diazo-5-oxo-l-norleucine (DON), 8-anilino-1-naphthalene sulfonic acid (ANS), 2,2′-(ethylenedioxy)bis(ethylamine), glutamine assay kit (Sigma), and all deuteriated solvent were procured from Sigma-Aldrich. Amberlite Ira 900 chloride ion exchange resins were obtained from Aldrich Chemical Co. Snake skin Dialysis membrane and all the materials required for cell culture study such as Dulbecco's modified Eagle's medium (DMEM), heat inactivated fetal bovine serum (FBS), Antibiotic-Antimycotic (100X) were obtained from Thermo Fisher Scientific. Trypsin-EDTA solution 1X (0.25% solution) was procured from Himedia. A549, HEPG2, and HEK 293, cells were bought from NCCS, Pune, India. All the primary and secondary antibody were purchased from Cell Signalling Technologies. All the experiment were performed using Milli-Q water. The critical aggregation concentrations (CAC) of TMAV were measured using a tensiometer (Jencon, India) by applying the Du Noüy ring method at 25 ± 0.1 °C in water.

Determination of critical aggregation concentration (CAC).

The critical aggregation concentration (CAC) of TMAV was determined by surface tension method using a tensiometer by applying the Du Noü y ring method at 25 ± 0.1 °C. A stock solution of TMAV (10 mg/mL) in water was prepared and the surface tension was measured for each diluted solution (having a specific concentration) prepared from the stock. The CAC value

was determined by plotting surface tension versus concentration of TMAV with an accuracy of ±2% in the triplicate experiments.

Transmission electron microscopy (TEM).

The TMAV solution in aqueous medium (5 μL) was deposited on a 300-mesh carbon coated copper grid and left for 1 min to adsorb. Filter paper was used to blot the excess solution. Negative staining of copper grid was done with freshly prepared uranyl acetate solution (1 μL, 1% w/v) and immediately, the excess solution was blotted with filter paper. Prior to taking the images, sample was dried for 4 h in a vacuum. The TEM images were taken in JEOL JEM 2010 microscope. Similarly, we have performed TEM study for the solution of HACD and **HACD-TMAV** conjugate without negative staining of uranyl acetate.

Field-emission scanning electron microscopy (FESEM).

FESEM images of TMAV and **HACD-TMAV** was captured on JEOL-6700F microscope. TMAV solution in pure water (4 μL) was drop cast on a piece of coverslip and dried overnight. Before taking images on a JEOL-6700F microscope, it was kept under the vacuum for a few hours. Similarly, FESEM study of **HACD-TMAV** conjugate was performed.

Dynamic light scattering (DLS) and zeta (ζ) potential measurement.

Dynamic Light Scattering (DLS) study was conducted to determine the mean hydrodynamic diameter (D_h) of TMAV in aqueous medium using Malvern Zetasizer S90 series. The surface charge of the TMAV and HACD in Milli-Q water was analyzed using the Zetasizer (Malvern Instruments, UK). To investigate the best weight ratio of TMAV and HACD to form **HACD-TMAV** conjugate, we have conducted DLS study of **HACD-TMAV** prepared by varying weight ratio of TMAV and HACD as mentioned above and their respective zeta (ζ) potential was measured.

Fluorescence microscopic study.

10 μL aqueous solution of HACD and **HACD-TMAV** conjugate was drop cast on a glass slide followed by overnight drying. The corresponding images were taken on a fluorescence microscope (Olympus IX83 inverted) at 40x magnification.

UV-visible study.

UV−vis study of TMAV was carried out using 8-anilino-1-naphthalenesulfonic acid (ANS) as the probe.[22] The solvent dependent UV−vis spectra of ANS (1×10^{-5} M) doped TMAV (0.5 mg/mL) were recorded on Agilent Cary 60 spectrophotometer. The solvents were varied from a non-self-assembled state (DMSO) to self-assembled one (water). The absorption spectrum of HACD was recorded on the same instrument. **HACD-TMAV** conjugate formation was followed by recording UV-vis spectra in a quartz cell (path length 10 mm). The temperature was fixed at 25 °C throughout the experiment by a Peltier thermostat.

FTIR study.

FTIR spectra were recorded on PerkinElmer Spectrum 100 FTIR spectrometer. Each of samples was mixed with potassium bromide separately and their respective KBr pellets were obtained by compressing the powders for 5-6 min on hydraulic press and the spectra were taken. The FTIR spectrum of TMAV in D_2O was recorded using 1 mm CaF2 cell.

Photoluminescence study.

Excitation dependent emission spectra of HACD (10 μg/mL) were recorded in Agilent Cary Eclipse luminescence spectrometer by varying λ_{ex} from 260 to 360 nm. The photoluminescence spectra of **HACD-TMAV** were recorded at a same concentration of HACD to ensure the conjugate formation. Furthermore, the relative fluorescence intensity (I/I_0) of **HACD-TMAV** conjugate in Milli Q as well as in media used during cellular internalization was studied for 8

days where, I_0 = original fluorescence intensity and I = fluorescence intensity at different days of **HACD-TMAV**, respectively.

Quantum yield (QY) measurement. Quantum yields are generally calculated with respect to an optically diluted standard fluorophore solution showing a well-known QY (ϕ_s). The QYs (ϕ_u) of the unknown fluorophore was measured by Parker-Rees method.

Here, A_u and A_s denoted the absorbance of unknown sample and the standard sample at the same excitation wavelength respectively. F_u and F_s denoted the area of the integrated fluorescence intensity for the unknown sample and known sample upon exciting at the same excitation wavelength respectively. A solution with similar absorbance (<0.1) was taken to measure the QY. n_u and n_s signify the refractive indices of the solvents in which the unknown and standard sample was prepared respectively. Here, quinine sulfate was chosen as the standard and dissolved in 0.1 M sulfuric acid (H_2SO_4) to measure its standard QY (ϕ_s) = 54.0%.

Cell culture.

$CD44^+$ A549 lung adenocarcinoma, $CD44^-$ HepG2 cell lines along with non-cancer cell line HEK293 were cultured in DMEM medium containing 10% FBS and antibiotics (100 mg/L streptomycin and 100 IU/mL penicillin) in culture flasks. Humidified condition (5% CO_2 and 37 °C) was maintained during the culture of mentioned cell line. Following 75% confluency, the cells were trypsinized and sub cultured as well as used for cellular experiments.

Cytocompatibility assay.

The cytocompatibility of the synthesized **HACD-TMAV** was enquired against $CD44^+$ A549 and $CD44^-$ HepG2 cancer cells along with the non-cancer cell line HEK 293 by MTT assay. In this assay, soluble tetrazolium gets reduced into insoluble formazan by the excreted mitochondrial

dehydrogenase from viable cells. The so obtained insoluble formazan was dissolved in DMSO to estimate the % of viable cells spectrophotometrically. Formazan formation is proportional to the quantity of alive cells. In this context, all the three cell lines (2×10^4 cells/well) were incubated in 96-well plates under humidified condition (5% CO_2 and 37 °C). Upon 70% confluency, the cells were treated with different concentrations of **HACD-TMAV** (2- 60 μg/mL) samples and incubated for 24-48 h. Following incubation with **HACD-TMAV**, the cells were washed with PBS and supplemented with fresh medium containing 10 μL of MTT (5 mg/mL in PBS) for 4 h. The formazan crystal so formed was solubilize using 100 μL DMSO and subjected to SpectraMax iD5 to record the respective absorbance at 570 nm. Next, the cell viability was calculated using the following equation 2. Similarly, cell viability was examined in $CD44^+$ Hep3B cancer cells.

% cell viability = (A_{570}(treated cells)-background)/A_{570}(untreated cells)-background) × 100 (2)

Characterization data.

^{1}H-NMR of TMAV (500 MHz, DMSO-d_6, 25 °C): δ (ppm) = 3.12-3.25 (m, 6H, Ph-C<u>H</u>$_2$), 3.26-3.35 (m, 6H, C<u>H</u>$_2$NH-CO), 3.37-3.51 (t, 6H, C<u>H</u>$_2$-NH_3^+), 3.53-3.72 (m, 24H, three different position of oxyethylene moiety), 4.80 (m, 3H, chiral proton of amino acid, 7.22-7.34 (m, 15H aromatic proton of phenyl alanine and 6H, amide), 8.39 (s, 3H, aromatic proton of trimesic acid).

Mass calculated for $C_{54}H_{78}N_9O_{12}$: 1041.5518; found:1042.4742 $[M+H]^+$.

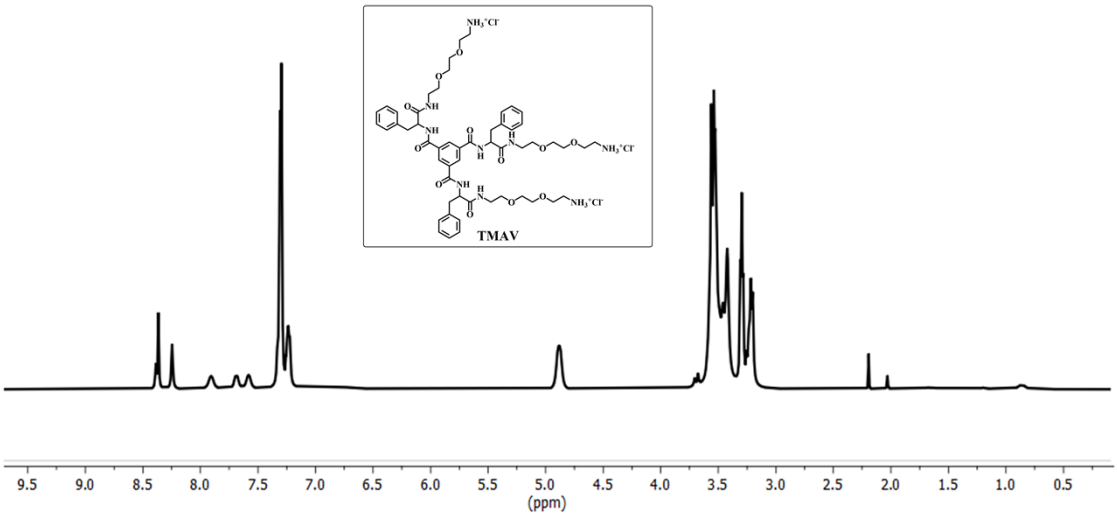

Fig. S1. ^{1}H-NMR spectrum of TMAV.

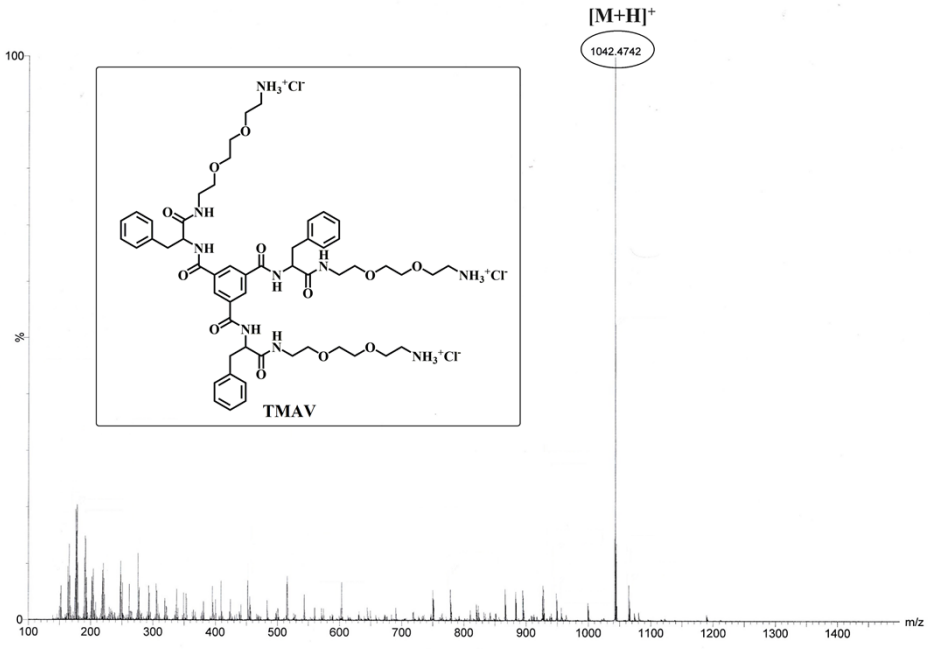

Fig. S2. Mass spectrum of TMAV.

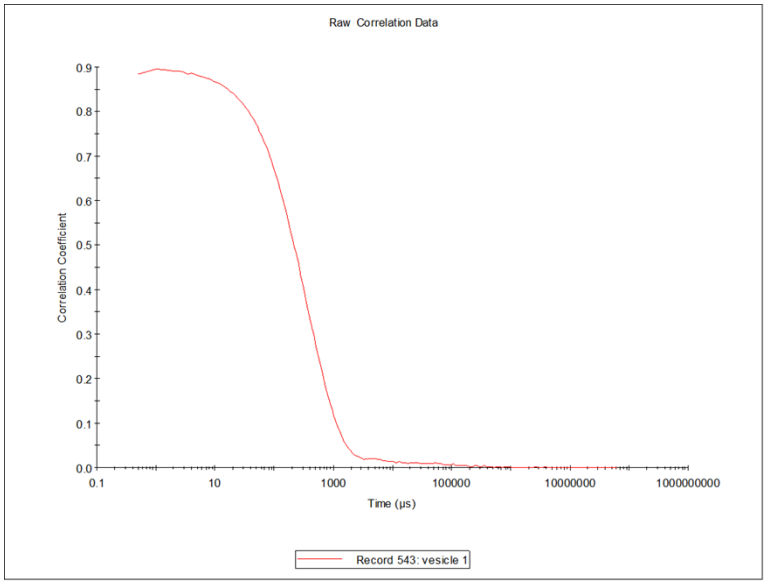

Fig. S3. DLS correlogram of TMAV vesicle.

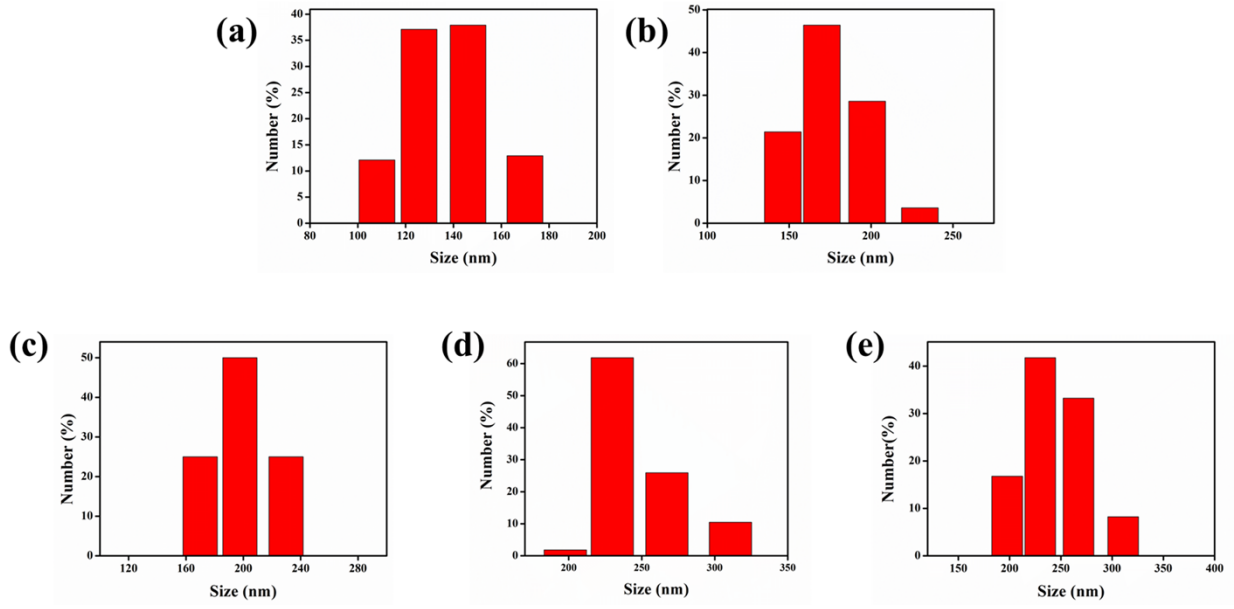

Fig. S4. DLS plots of particle size distribution of **HACD-TMAV** conjugate at different weight ratios (a) 1:0.1, (b) 1:0.2, (c) 1:0.3, (d) 1:0.5, (e) 1:1 (w/w) of TMAV and HACD, respectively.

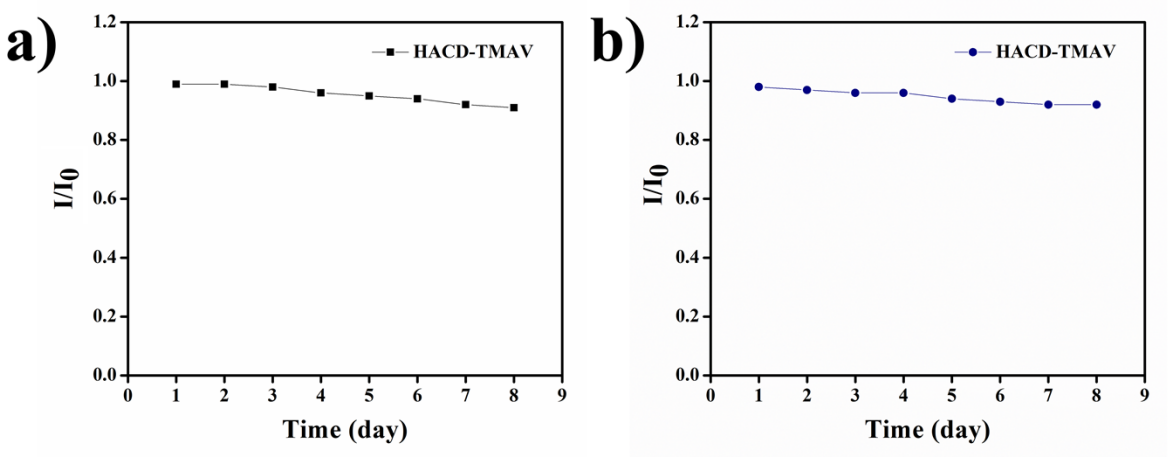

Fig. S5. Relative fluorescence intensity plot of **HACD-TMAV** over time in a) Milli Q, b) media used during cellular internalization.

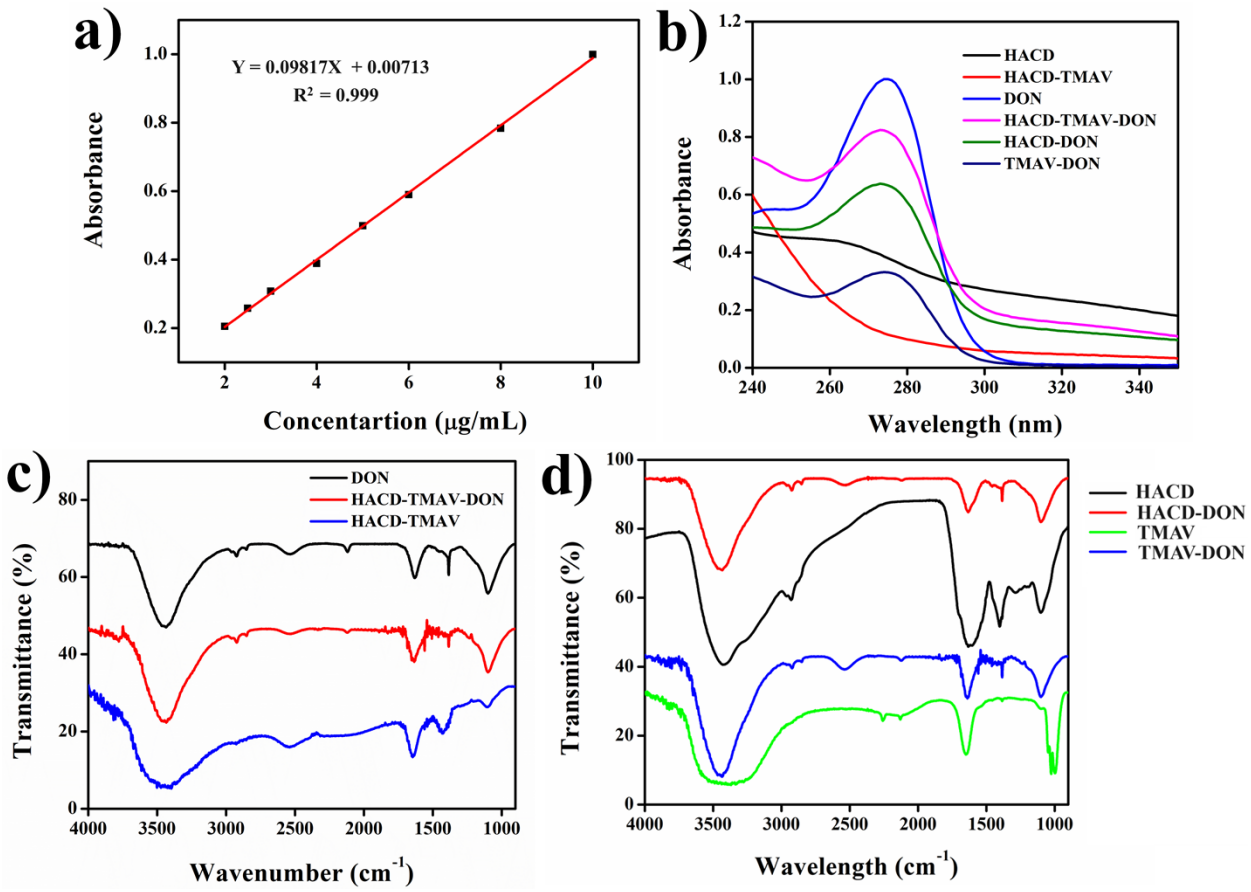

Fig. S6. (a) Standard calibration curve of DON, (b) UV-vis spectra of **HACD-TMAV**-DON, HACD-DON, TMAV-DON, native DON, (c) FTIR spectra of DON, **HACD-TMAV** and **HACD-TMAV**-DON, (d) FTIR spectra of HACD, TMAV, HACD-DON and TMAV-DON.

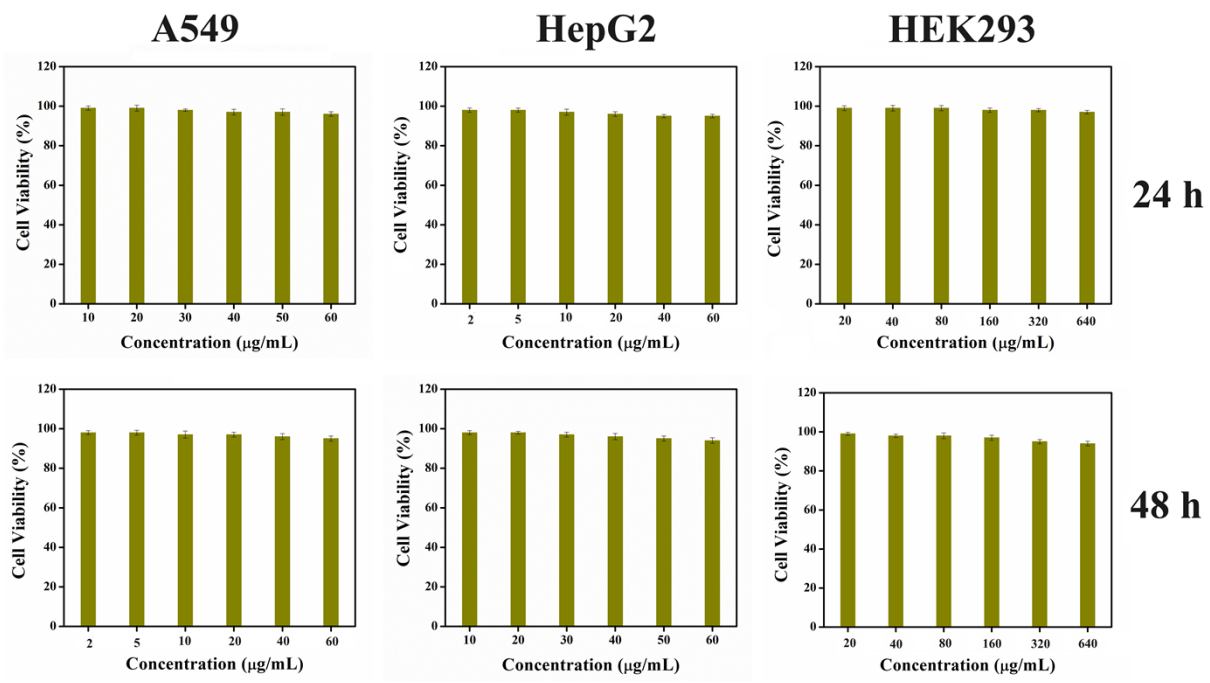

Fig. S7. Cytocompatibility of **HACD-TMAV** conjugate against A549, HepG2, HEK 293 cells with increasing concentrations for 24 and 48 h as observed from MTT assay. Percent experimental errors are within approximately ± 3% in triplicate experiments.

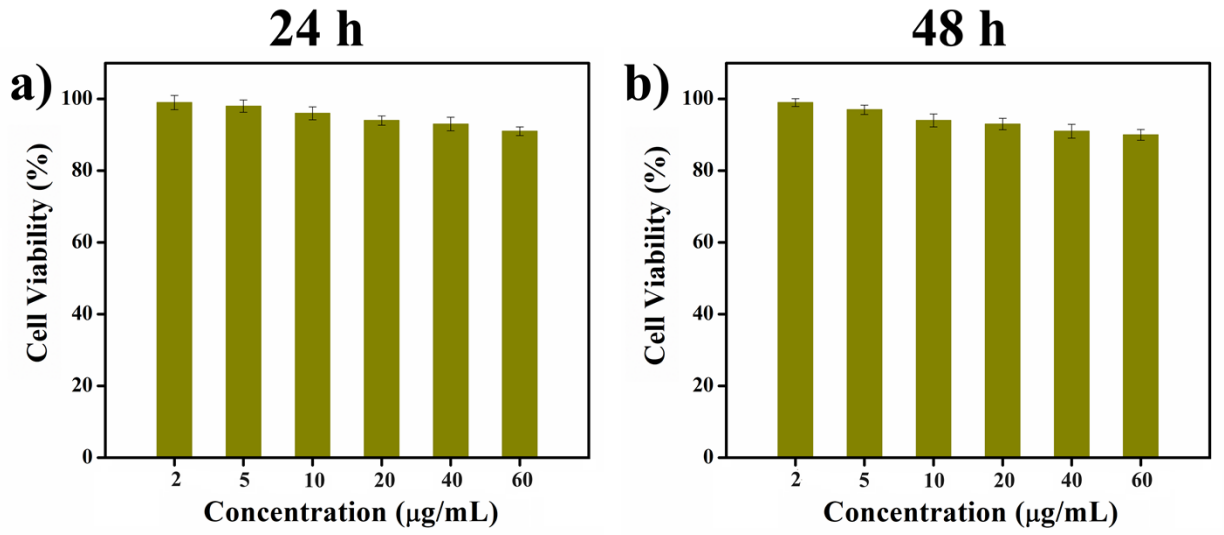

Fig. S8. Cytocompatibility of **HACD-TMAV** conjugate against Hep3B cells with increasing concentrations for 24 h and 48 h, as observed from MTT assay. Percent experimental errors are within approximately ± 3% in triplicate experiments.

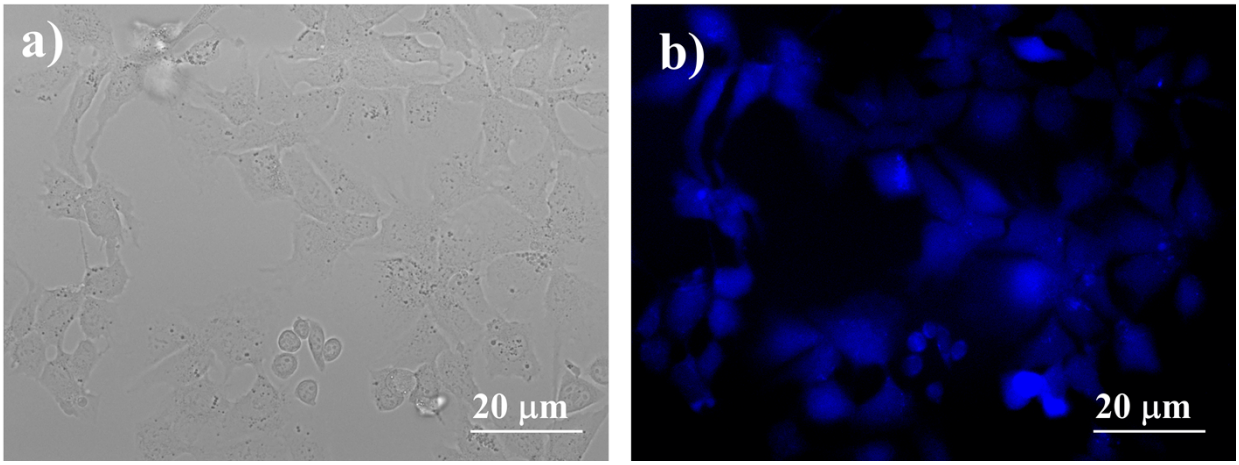

Fig. S9. (a) Bright field, (b) fluorescence images of Hep3B cells incubated for 6 h with **HACD-TMAV** conjugate (200 μg/mL). Scale bars correspond to 20 μM.

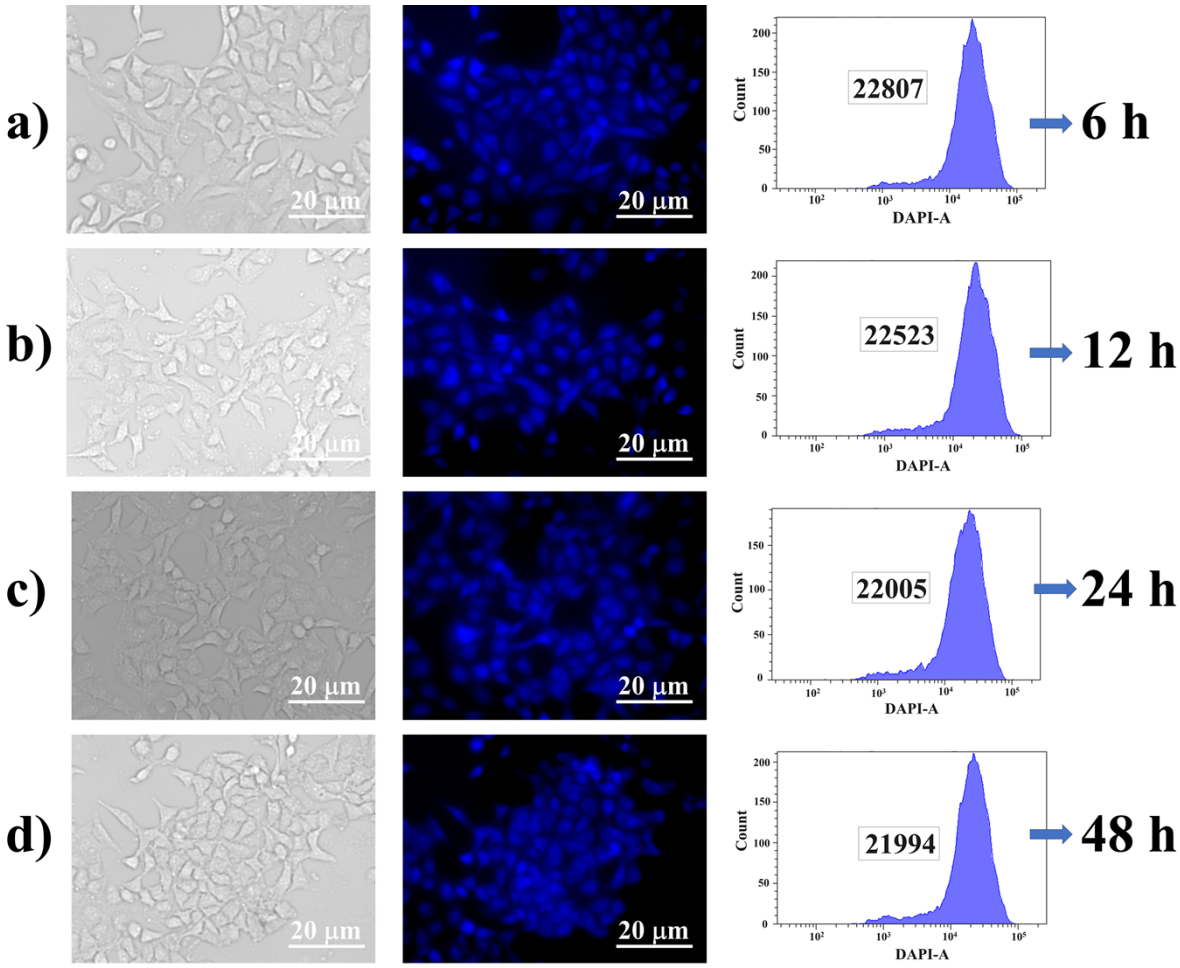

Fig. S10. Brightfield, fluorescence microscopic images and corresponding flow cytometric analysis plots of A549 cells upon incubation with **HACD-TMAV** (200 µg/mL) for a) 6 h, b) 12 h, c) 24 h, and d) 48 h. The mean fluorescence intensity values are given in the insets. Scale bars correspond to 20 µm.

Table S1. IC_{50} value for HACD-DON and **HACD-TMAV**-DON.

Drug loaded Nano-Carrier	**IC_{50} value (μg/mL)**
HACD-DON	54.7
HACD-TMAV-DON	20.0

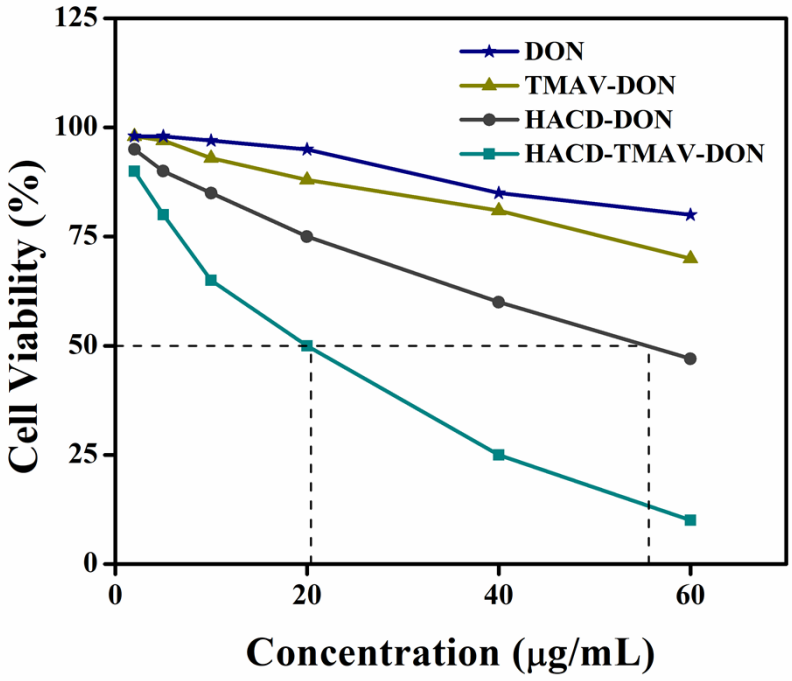

Fig. S11. IC_{50} determination of HACD-DON and **HACD-TMAV**-DON.

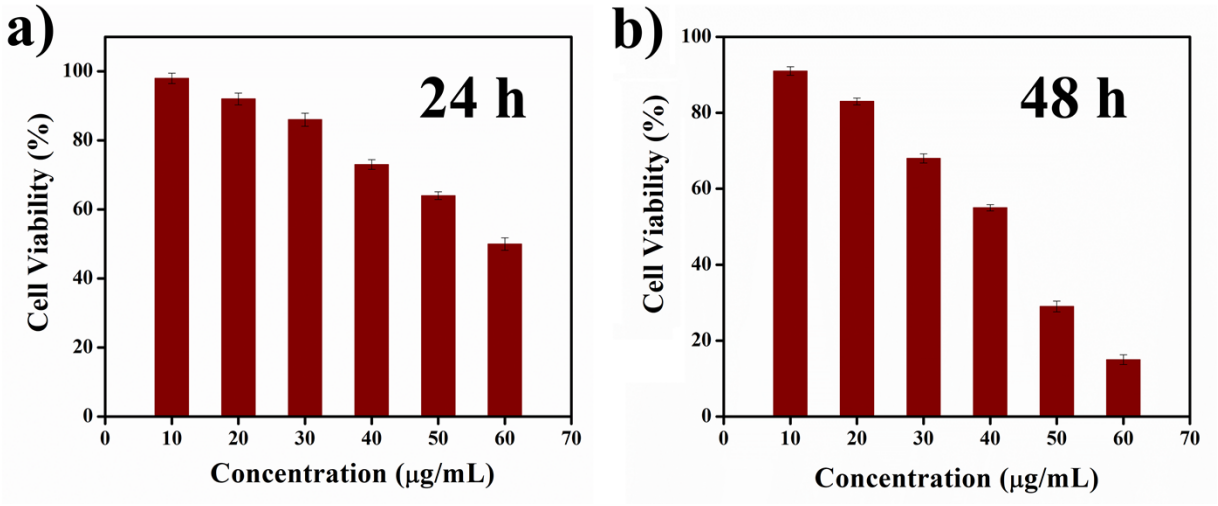

Fig. S12. Cytotoxic potential (determined by MTT assay) of **HACD-TMAV**-DON with increasing concentrations towards Hep3B cells, for 24 h – 48 h. Percent experimental errors are within approximately ± 3% in triplicate experiments.

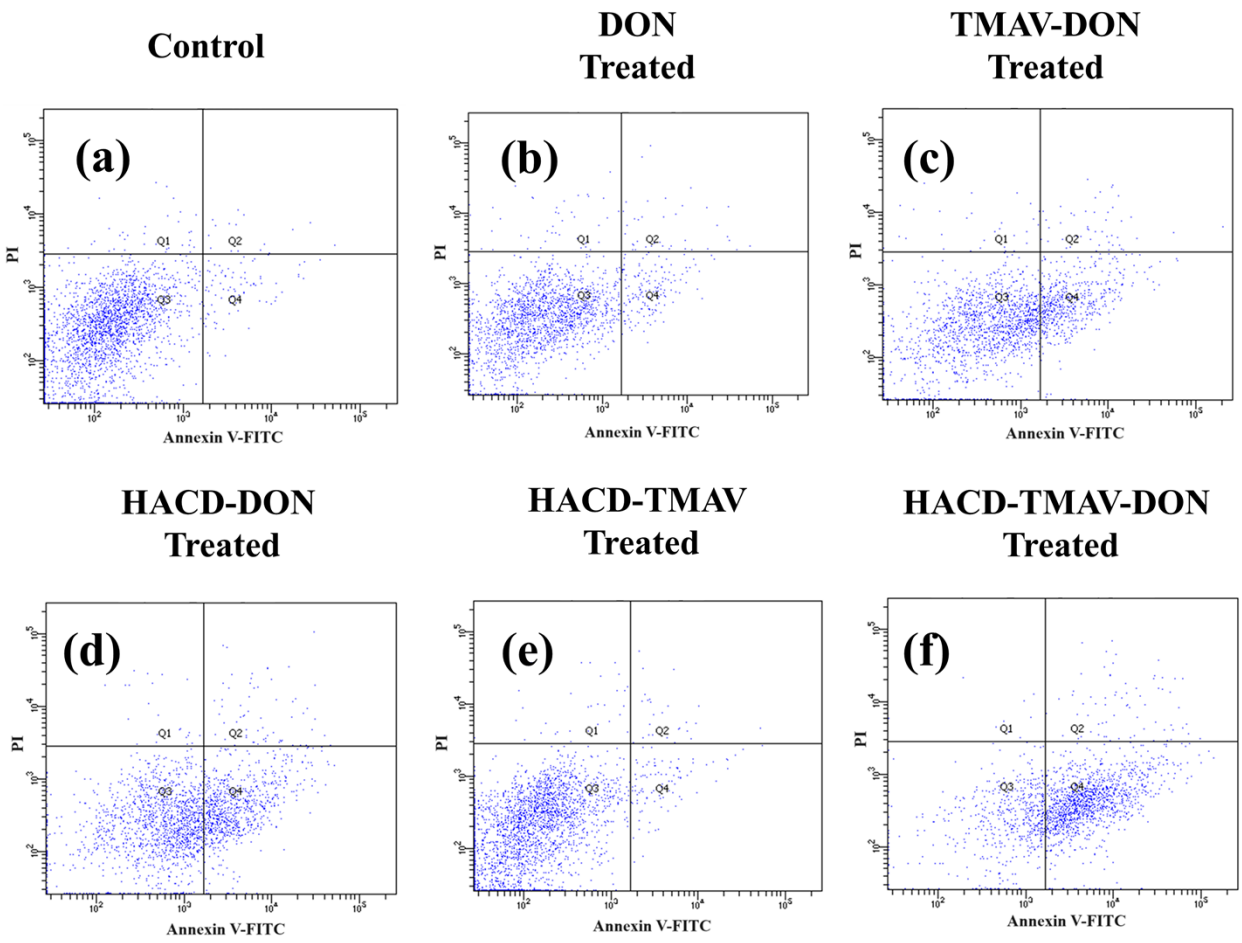

Fig. S13. Flow cytometric analysis of apoptosis in A549 (a) control cells, as well as cells treated with (b) native DON, (c) TMAV-DON, (d) HACD-DON (e) **HACD-TMAV** and (f) **HACD-TMAV**-DON at a concentration of 60 μg/mL for 24 h.

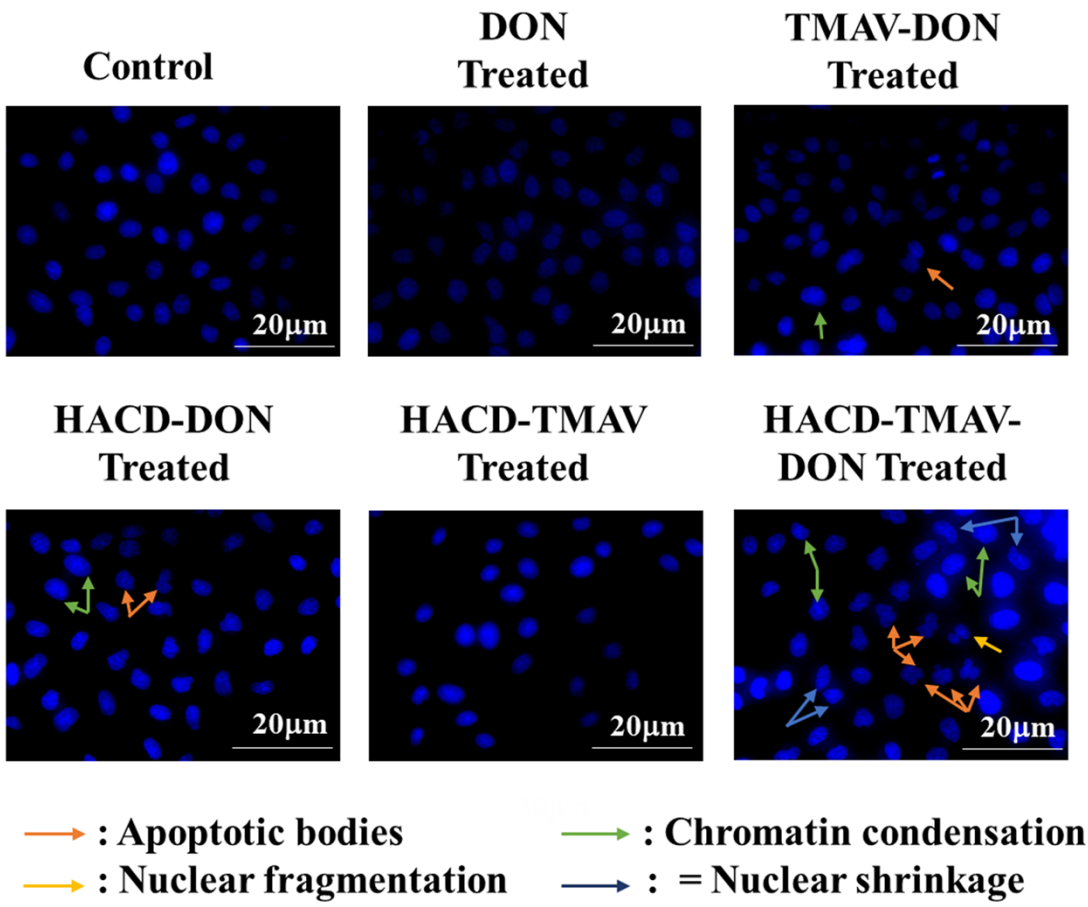

Fig. S14. Nuclear staining of A549 cells with Hoechst 33342 dye following incubation with native DON, TMAV-DON, HACD-DON, **HACD-TMAV**, and **HACD-TMAV**-DON for 36 h.

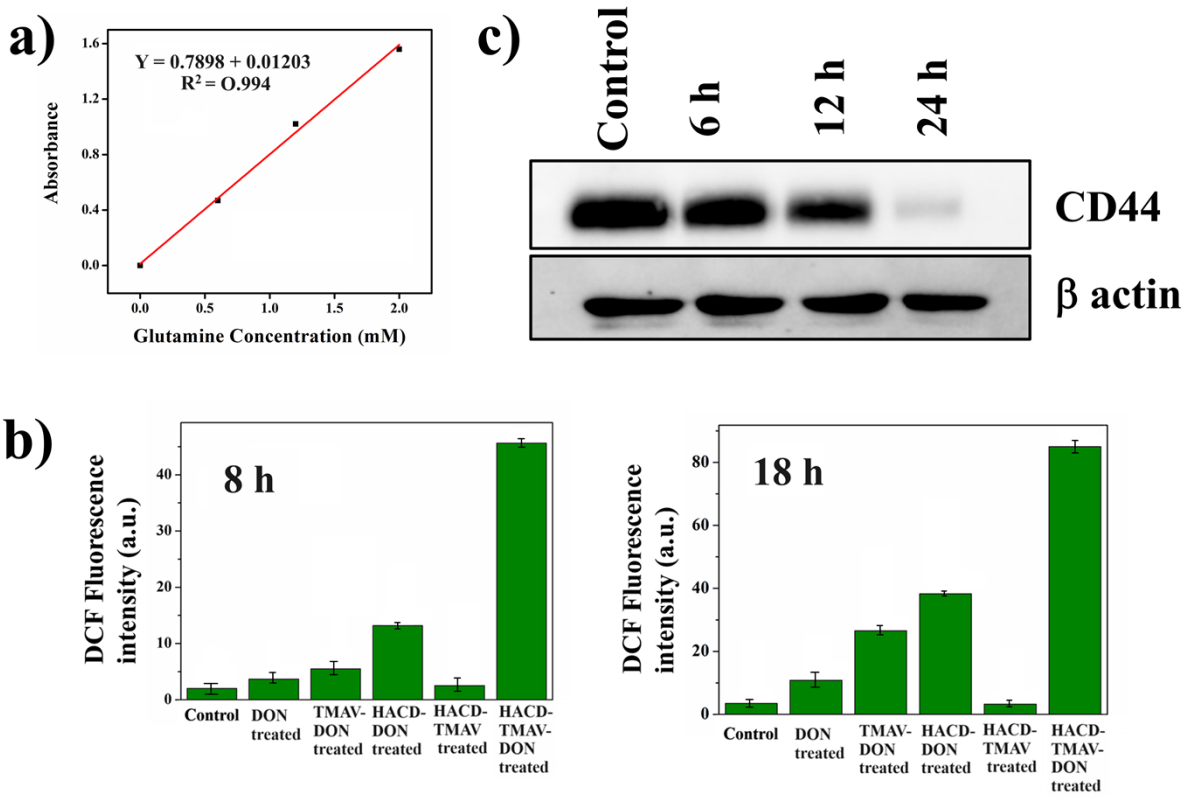

Fig. S15. (a) Calibration curve of Glutamine (dissolved in water), (b) Comparative analysis of the intracellular ROS level in A549 cells as indicated by DCF green fluorescence intensity following incubation with **HACD-TMAV**, native DON, TMAV-DON, HACD-DON and **HACD-TMAV**-DON at 60 µg/mL of each formulation for 8 h and 18 h and c) Time-dependent immunoblot analysis, treating A549 cells with **HACD-TMAV**-DON for 6, 12, and 24 hours. β-actin levels are shown as loading control.

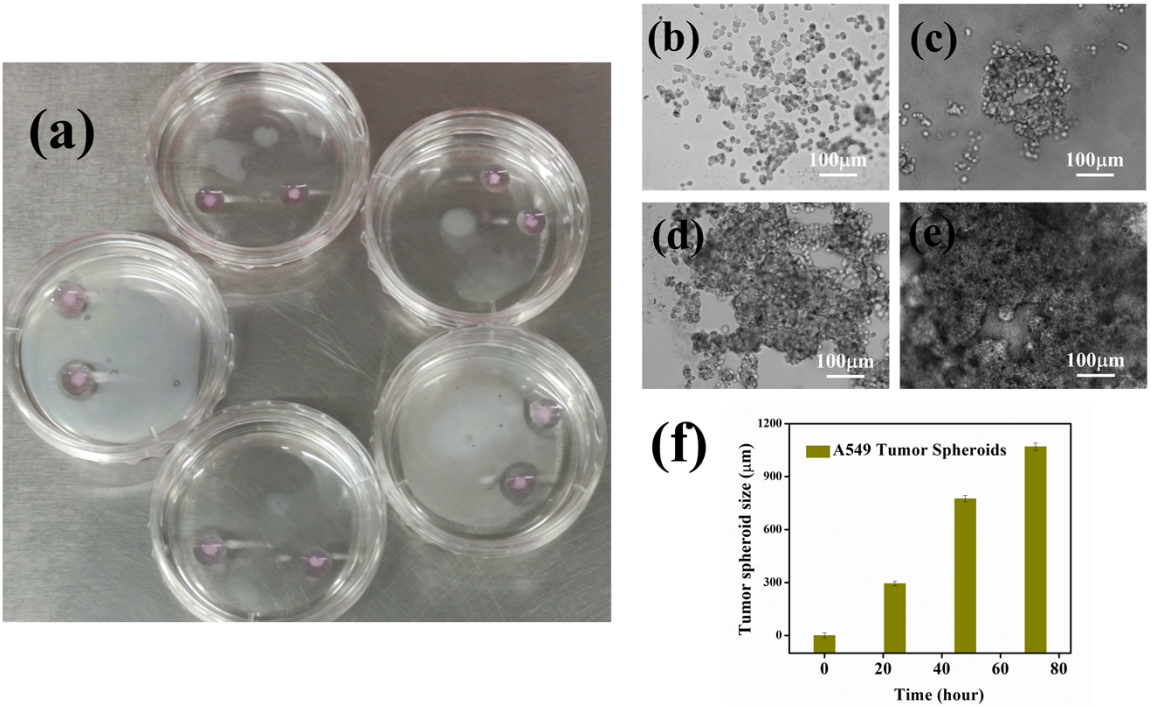

Fig. S16. (a) Hanging drop method of developing 3D tumor spheroids in 35 mm culture plate; bright-field images of 3D tumor spheroids formed by culturing A549 cells in 3D culture platform for (b) 0 h, (c) 24 h (c) 48 and (e) 72 h; (f) time-course monitoring of tumor spheroid diameter.

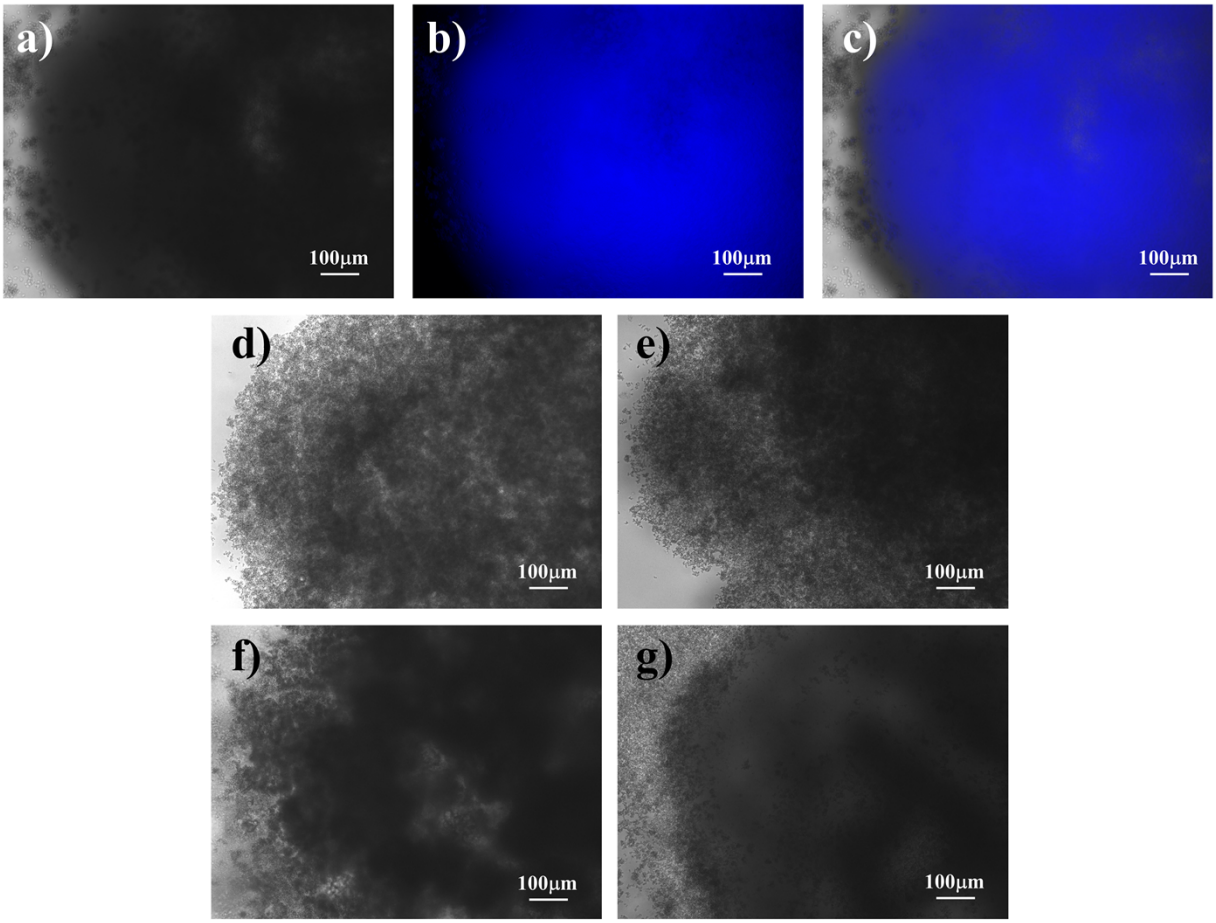

Fig. S17. (a) Bright field, (b) fluorescence (c) merged image of 3D tumor spheroids of A549 cells after incubation for 6 h with **HACD-TMAV**. Bright field images of 3D tumor spheroids formed by culturing A549 cells upon incubation with **HACD-TMAV** for (b) 0 h, (c) 24 h (c) 48 and (e) 72 h.

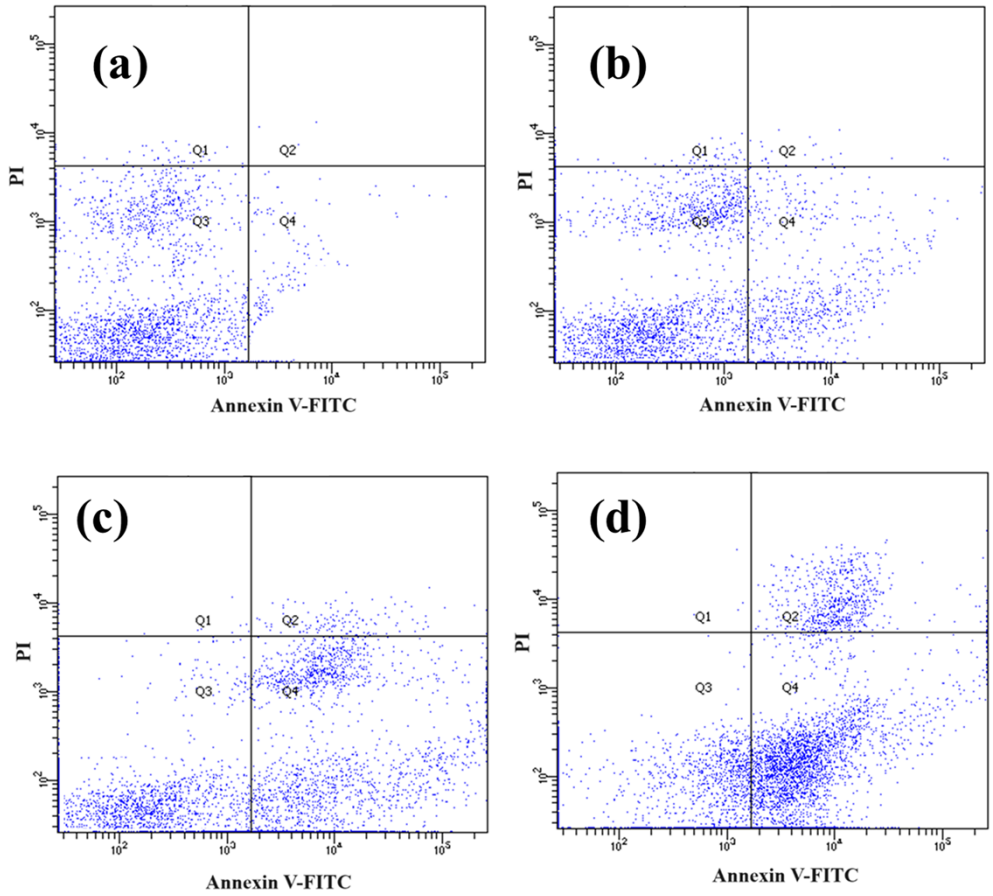

Fig. S18. Flow cytometric analysis of apoptosis in (a) control tumor spheroids and in those treated with **HACD-TMAV-**DON at a concentration of 60 µg/mL for (b) 24 h, (c) 48 h, (d) 72 h. Treatment of the tumor spheroids with **HACD-TMAV**-DON was conducted in triplicates.

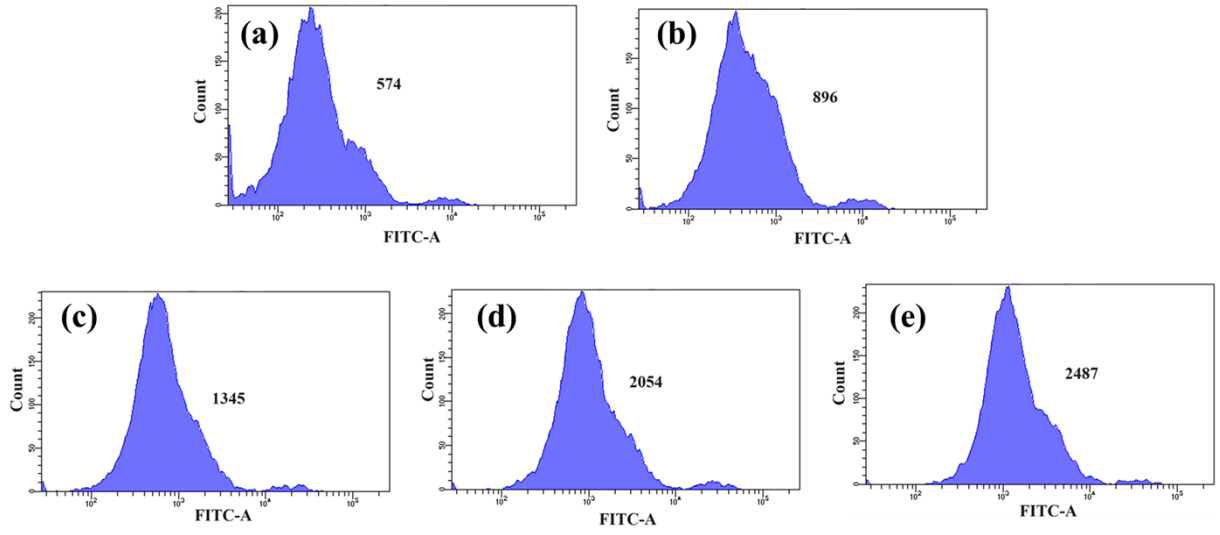

Fig. S19. Flow cytometric analysis of intratumorally ROS generation as indicated by DCF fluorescence in (a) control tumor spheroids and in those following incubation with **HACD-TMAV**-DON for (b) 6 h, (c) 12 h, (d) 24 h and (e) 48 h. Treatment of the tumor spheroids with **HACD-TMAV**-DON was conducted in triplicates.